Revisiting the O-O Bond Formation through Outer Sphere Wa- ter Molecules vs Bimolecular Mechanism in Water Oxidation Catalysis (WOC) by Cp*Ir-based Complexes

Farhan Pasha, Sai V C Vummaleti, Theodorus de Bruin, Albert Poater, Jean Basset

Revisiting the O-O Bond Formation through Outer Sphere Water Molecules vs Bimolecular Mechanism in Water Oxidation Catalysis (WOC) by Cp*Ir-based Complexes

Fahran A. Pasha,[†] Sai V. C. Vummaleti,[†] Theodorus de Bruin,[§] Albert Poater,[†,‡,*] and Jean M. Basset[†,*]

[†] *KAUST Catalysis Center, Physical Sciences and Engineering Division, King Abdullah University of Science and Technology, Thuwal 23955-6900, Saudi Arabia*

[§] *IFP Energies nouvelles, 1-4 Avenue de Bois Préau, 92852, Rueil-Malmaison, France*

[‡] *Institut de Química Computacional i Catàlisi and Departament de Química, Universitat de Girona, Campus Montilivi, 17003 Girona,* Catalonia, Spain

KEYWORDS: water splitting, DFT, mechanism, iridium, oxygen evolution, O-O coupling, water oxidation catalysis

Herein we present a detailed computational investigation of the mechanistic aspects of the water oxidation catalysis (WOC) for iridium based catalysts, Cp*Ir-$\mathbf{L}_{x=1-4}$, (where Cp* = pentamethylcyclopentadiene; $\mathbf{L_1}$ = bph = bi-phenyl; $\mathbf{L_2}$ = phpy = 2-phenylpyridine; $\mathbf{L_3}$ = bpy = 2,2′-bipyridyl; and **L4** = bnql = benzo[n]quinoline or 1-naphthoquinoline). Our density functional theory (DFT) calculations not only confirmed that the O-O coupling step is the rate-limiting step as expected, but also provided useful insights about the number of water molecules involved in the catalytic cycle, which is under immense debate from a kinetic stand point. To test the effect of the metal environment, we tuned the ligands choosing four ligands (L_1-L_4) holding four kinds of chelation: C-C, N-C, N-N and C-N' ($\mathbf{L_1}$ = bph = bi-phenyl; $\mathbf{L_2}$ = phpy = 2-phenylpyridine; $\mathbf{L_3}$ = bpy = 2,2-bipyridyl; and $\mathbf{L_4}$ = bnql = benzo[n]quinoline or 1-naphthoquinoline) ligands, respectively. A screening analysis of the potential energy surface revealed the water oxidation mechanism together with the optimum number of water molecules, concluding that three water molecules are mandatory for the right recipe, and that a highly positive iridium oxo center with high oxidation state (Ir(V)) pulls the electron density from lone pair of oxo oxygen and O center shows positive density. The most external water molecule or second OH_2 (**W2**) becomes nucleophilic while approaching the iridium center because of the proton abstraction by another water molecule (**W3**), and the nucleophilic water (**W1**) attacks the electrophilic oxygen facilitating the O-O bond formation. Moreover, the bimolecular mechanism for the O-O bond step was also calculated for terms of comparison. This study reveals that high cationic character of the metal is helpful for the O-O coupling.

Water oxidation catalysis (WOC) is a subject of great scientific interest during last couple of decades owing to its potential application to make renewable energy carriers.[1] Our limited understanding of WOC, which is considered to be a difficult process in terms of chemical or electrochemical driving force, is the main hurdle in realizing this alternative energy scheme.[2] The one electron process ($HO^* + H^+ + e^-$) occurs at E=2.848 V vs NHE, while the two electron process and formation of H_2O_2 has a barrier about E=1.776 V vs NHE.[3] The most widely studied four electron oxidation $2H_2O \rightarrow O_2 + 4e^- + 4H^+$ has a barrier about E=1.236 V vs RHE.[4] Beside dynamics, the kinetics of these reactions is very slow. However, in recent years, the hydrogen evolution reaction (HER) has been widely addressed and a few major breakthroughs have been realized.[5] In the same line, several homogeneous catalysts have been reported for the oxygen evolution reaction (OER).[6] Even though Ru-based catalysts are usually common as water oxidation catalysts,[7,8] in 2008 McDaniel et al reported the first mono nuclear iridium water oxidation catalyst.[9] Furthermore, Hull et al reported Cp*Ir complexes (Cp* is pentamethylcyclopentadiene) as efficient water oxidation catalysts,[10] and Grotjahn et al enlarged the ligand environment on iridium suitable for WOC.[11] Recently, Joya et al described the first example of the immobilization of Cp*Ir based molecular complexes (having -COOH and $-PO_3H_2$ type surface anchoring units) on conducting substrate for electrochemical water oxidation catalyst,[12] followed by a recent heterogenization by means of TiO_2 by Macchioni et al.[13] From a mechanistic point of view, the active catalytic species of Cp*Ir based catalysts is the cationic metal-oxo complex (**Cat**, Figure 1). Coordination of *n* water molecules (where *n* = 1-4) to species **Cat** leads to coordination intermediate (**Int1**), which subsequently undergoes O-O coupling step to produce Cp*Ir-peroxo complex (**Int2**),[14,15] through transition state **TS**. Finally, PCET (proton-coupled electron

transfer) step followed by the addition of a new water molecule to help to **Int2** release the O_2 molecule.[12,16,17]

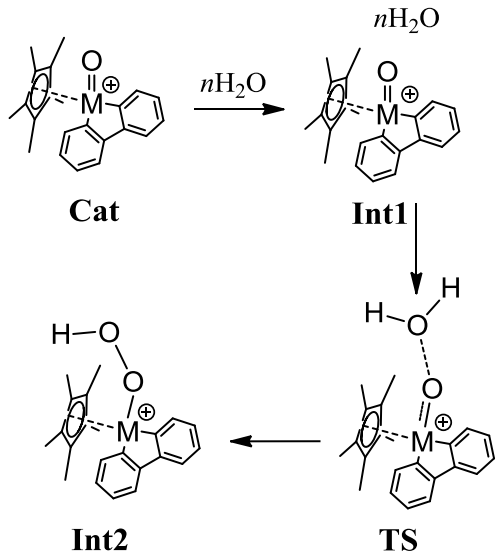

Figure 1. Structural scheme of the key steps during water oxidation catalytic cycle for an exemplary metal-organic complex.

In homogeneous water oxidation studies using Cp*Ir-based molecular catalysts,[18] Ce(IV) in the form of cerium ammonium nitrate (CAN) is the most commonly used chemical oxidant or one electron catalyst activator (E° ~ 1.61 V vs. NHE), and might assist the O-O bond formation, as well.[19] Addition of quantitative amount of CAN into catalytic solution (4 eq. to generate one O_2 molecule) induces the catalyst activation by the abstraction of electrons, and the overall water oxidation reaction can be presented as in Scheme 1.

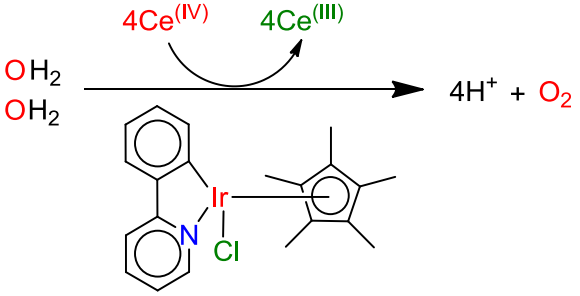

Scheme 1: Water oxidation reaction scheme using $Ce^{(IV)}$ as one electron donating agent for Cp*Ir-based molecular catalysts.

Besides this knowledge, the exact mechanism of O-O coupling,[20] the reaction driving forces and the role of hydrate cluster or the number of water molecules involved in molar water oxidation is still under debate. On a broader scope, the electronic spin densities and the spin cross over during the reaction remain unexplored. To fill this gap, in the present study, we aim to investigate and probe the details of the O-O bond formation in WOC for a family of Cp*-Ir based complexes and to establish a comprehensive framework using DFT[21] to facilitate ligand/catalyst designing. The current study takes into account a series of four model catalysts derived from Cp*Ir architecture (Figure 2), $\mathbf{L_{1\text{-}4}}$, for water oxidation; where $\mathbf{L_1}$ is a C-C bis phenyl (bph), $\mathbf{L_2}$ is a C-N based 2-phenylpyridine (phpy) ligand, $\mathbf{L_3}$ is a N-N based 2,2′-bipyridyl (bpy) and $\mathbf{L_4}$ is benzo[h]quinoline or 1-naphthoquinoline (bnql).[22] To point out that Cp*Ir-$\mathbf{L_1}$ complex is an in silico catalyst and has not been synthesized yet.

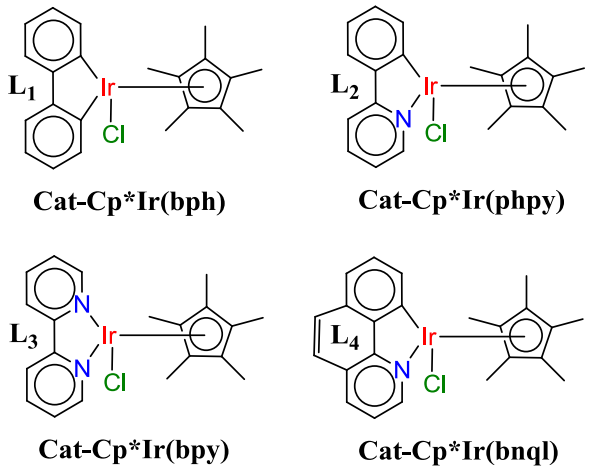

Figure 2. Chemical structures of the studied molecular iridium catalyst series Cp*Ir, $\mathbf{L_{1\text{-}4}}$, for water oxidation.

Results

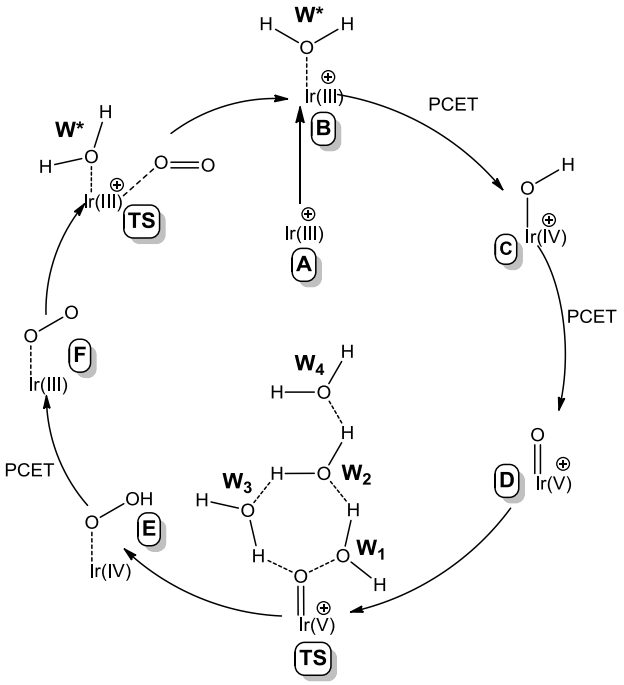

Figure 3. The catalytic cycle for water oxidation by Cp*Ir based single-site molecular catalyst.

Figure 3 presents the plausible general scheme of water oxidation catalytic cycle mediated by Cp*Ir based catalysts. Bearing the overall catalytic cycle in Figure 3, with the aim of rationalizing the water oxidation process. Going into the details, the reaction starts from the formation of cationic Cp*Ir(III) complex (**A**) by the release of Cl ligand. Next, coordination of a water molecule to the metal center in **A** leads to the formation of complex **B** (**W***), which undergoes a PCET step to form **C** bearing iridium in $Ir^{(IV)}$ oxidation state. Then, complex **C** undergoes a second PCET step to form the metal-oxo complex **D** (**Cat**, Figure 1). It is worth mentioning here that the oxidation state V for iridium exhibits a neutral metal center with ligand $\mathbf{L_1}$, while a positively charged metal center with ligands $\mathbf{L_{2\text{-}4}}$, being +1 with $\mathbf{L_2}$ and $\mathbf{L_4}$, while +2 with $\mathbf{L_3}$. As reported in the literature, species **D** is the active catalytic species to face the O···O bond formation.

The next step, complex **D→E**, involves a transition state (**TS**) where the oxygen of a water molecule (**W1**) attacks the oxo moiety in **D** to give peroxo complex **E**, which then undergoes a couple of PCET steps to form complex **F**. Finally, complex **F** may regenerates **B** by coordinating a new water molecule (**W***) and the subsequent release of O_2. , and thus closing the catalytic cycle. In a different route, the O_2 release from **F** together with the metal reduction step regenerates catalyst **A**.

There are two important aspects that must be taken in account for the active catalytic metal-oxo complex **D**: first, the number of active water molecules around the oxo moiety which will be discussed in the next section; second, the most stable electronic ground state of **D**, i.e., singlet (S) or triplet (T) spin states. Thus, we center our efforts in rationalizing the step **D→E** corresponding to the O···O bond formation. For the sake of simplicity, in the following sections, we relabel complexes **D** and **E** as **Cat** and **Int2**, respectively, according to Figure 1.

Table 1. Relative stability of singlet (S) and triplet (T) ground states of metal-oxo species $\mathbf{L_x}$-**Cat** for the studied iridium catalyst series Cp*Ir-$\mathbf{L_{x=1\text{-}4}}$. Energies are given in kcal mol^{-1} relative to 'S' spin state.

	Gas-phase		Solvent-phase	
Species	ΔE_{gas}	ΔG_{gas}	ΔE_{sol}	ΔG_{sol}
$\mathbf{L_1}$-$\mathbf{Cat^S}$	0.0	0.0	0.0	0.0
$\mathbf{L_1}$-$\mathbf{Cat^T}$	-7.9	-8.8	-4.6	-5.5
$\mathbf{L_2}$-$\mathbf{Cat^S}$	0.0	0.0	0.0	0.0
$\mathbf{L_2}$-$\mathbf{Cat^T}$	-6.9	-8.6	-5.1	-13.7
$\mathbf{L_3}$-$\mathbf{Cat^S}$	0.0	0.0	0.0	0.0
$\mathbf{L_3}$-$\mathbf{Cat^T}$	-11.1	-12.2	-8.4	-20.5
$\mathbf{L_4}$-$\mathbf{Cat^S}$	0.0	0.0	0.0	0.0
$\mathbf{L_4}$-$\mathbf{Cat^T}$	-7.3	-9.3	-5.5	-14.8

ΔE is the electronic energy and ΔG is the Gibbs energy.

Table 1 reports the detail energetics (both gas-phase and solvent-phase electronic energies (ΔE) as well as Gibbs energies (ΔG)) of singlet and triplets state of metal-oxo complex $\mathbf{L_x}$-**Cat1** for the studied catalyst series Cp*Ir-$\mathbf{L_{x=1\text{-}4}}$. Although we presented the detailed energetics, here and in the following sections, we discuss only the solvent-phase free energies (ΔG_{sol}) as they are more reliable. It is clear from Table 1 that for complex $\mathbf{L_x}$-**Cat1**, the triplet ground state is more stable the singlet state. In detail, the presented ΔG_{sol} favors the triplet ground state by -5.5, -13.7, -20.5 and -14.8 kcal mol^{-1} for the catalysts bearing $\mathbf{L_1}$, $\mathbf{L_2}$, $\mathbf{L_3}$, and $\mathbf{L_4}$, respectively. Additionally, singlet-triplet energy differences in Table 1 suggest that the entropic contribution is not significant and counts to only 1-2 kcal mol^{-1}. On the other hand, the presented ΔE_{sol} indicates a narrowing of gap between stability of singlet and triplet states by 2-3 kcal mol^{-1}, A point worth to be noted here that the inclusion of thermal corrections into ΔE_{sol} energies significantly increases the singlet and triplet energy gap for complex $\mathbf{L_x}$-**Cat1** with ligands $\mathbf{L_2}$, $\mathbf{L_3}$, and $\mathbf{L_4}$ (9.0-12.0 kcal mol^{-1}), while with ligand $\mathbf{L_1}$ the gap is increased only by 1.0 kcal mol^{-1} because of its overall neutral character.

A recent DFT based mechanistic study of water oxidation catalysis for half-sandwich iridium complexes (bearing Cp*Ir framework) was reported by Eisenstein et al.[22] This study suggested the O-O coupling is the rate limiting step. Additionally, they proposed a lowest energy pathway for the formation of peroxo complex where one proton from the water molecule coordinated to the metal-oxo complex is transferred to a second water molecule, which subsequently transfers one proton to the oxo moiety (β-oxygen to the α-oxygen). The reevaluation of the reaction pathway described by Eisenstein et al reveals that the key transition state fails in the description of the O-O coupling step, as the transition state allows only the H transfer from the β-oxygen to the α-oxygen, assisted by a water molecule. Furthermore, the O···O bond length in the transition state was reported to be only 1.5 Å which is extremely short, and belongs to a true O-O bond rather than an O···O coupling transition state.

In this section, we revisited the mechanism for the crucial O-O coupling step by placing *n* number of active water molecules (where *n* = 2-4) around the metal-oxo complex **Cat**.[22] Since the number of coordinated water molecules to the metal-oxo complex **Cat** significantly affects the gap between the stable electronic ground states, we calculated the whole reaction profile for both S and T states. For this, we chose catalyst Cp*Ir-$\mathbf{L_2}$ as a reference system and reported the details of energetics for the O-O coupling step with respect to the water coordinated metal-oxo intermediate in S state ($\mathbf{Int1^S}$, ΔE_{gas} or ΔG_{gas} = 0.0 kcal mol^{-1}) (Table 2). Going into the details, complex $\mathbf{L_2}$-**Cat** is still more stable in triplet ground state (ΔE_{gas} = 7.0 kcal mol^{-1} and ΔG_{gas} = 9.0 kcal mol^{-1}) even in presence of two, three and four water molecules. Similarly, water coordinated first intermediate is found to be more stable in triplet ($\mathbf{L_2}$-$\mathbf{Int1^T}$) than singlet ground state ($\mathbf{L_2}$-$\mathbf{Int1^S}$) (ΔE_{gas} = 2.0-4.0 kcal mol^{-1}

and ΔG_{gas} = 5.0-6.0 kcal mol^{-1}). On the other hand, the lowest in energy transition state for the O-O coupling displayed always closed shell singlet as a ground state (**L_2-TS^S**). On the other hand, the transition state for the O-O coupling step always displayed the stable singlet ground state (**L_2-TS^S**). Our efforts to locate the transition state in triplet and quintuplet states (**TS^T** and **TS^Q**, respectively) were not successful. Therefore, we performed single point energy calculations with triplet ground state on the optimized geometries of singlet ground state, and in any case our results indicate that the triplet state is less stable by 3.0 kcal/mol confirming the stability of singlet ground state.

Table 2. Relative energies of singlet (S) and triplet (T) ground states of key intermediates of the water oxidation catalytic cycle for Cp*Ir-L_2 catalyst in the presence of *n* number of water molecules (*n*=2–4). Energies are given in kcal mol^{-1} relative to species **L_2-$Int1^S$($2H_2O$)**.

	Gas-phase					
H_2O	n=2		n=3		n=4	
Species	ΔE_{gas}	ΔG_{gas}	ΔE_{gas}	ΔG_{gas}	ΔE_{gas}	ΔG_{gas}
L_2-Cat^S	25.7	11.5	30.3	16.6	29.1	19.2
L_2-Cat^T	18.8	2.9	23.4	8.1	22.2	10.6
L_2-$Int1^S$	0.0	0.0	0.0	0.0	0.0	0.0
L_2-$Int1^T$	-4.4	-5.8	-2.2	-5.0	-2.4	-5.0
L_2-TS^S	25.7	25.3	24.4	23.8	22.0	24.9
L_2-$Int2^S$	3.1	5.0	10.5	13.2	11.7	16.6

The calculated gas-phase free energy barriers ΔG_{gas} for the O-O coupling step follows the trend: **L_2-TS^S($2H_2O$)** > **L_2-TS^S($3H_2O$)** < **L2-TS^S($4H2O$)** with energies 25.3 > 23.8 < 24.9 kcal mol^{-1}, respectively.

The data reveal that the third water molecule reduces the **L_2-$Int1^S$($3H_2O$)** → **L_2-TS^S($3H_2O$)** barrier (ΔE_{gas}) by 1.3 kcal mol^{-1}, because the added water molecule (**W_3**) is helping to polarize the molecule (**W_2**) which is abstracting a proton from water molecule (**W_1**), and consequently the water molecule (**W_1**) making an O-O peroxo bond with the oxo moiety. The two water molecule system lacks this polarization, which is translated into a higher barrier for the O-O coupling.

Figure 4 presents the reaction energy profile for the O-O coupling step mediated by iridium system bearing ligand **L_2** with two water molecules Cp*Ir-**L_2($2H_2O$)**.[22] The first intermediate in singlet ground state (**L_2-$Int1^S$($2H_2O$)**) was considered as the energy reference. The intermediate triplet ground state (**L_2-$Int1^T$($2H_2O$)**) was found to be 5.8 kcal mol^{-1} (ΔG_{gas}) more stable than the singlet state. The transition state which leads to the formation of the O-O bond (**L_2-TS^S($2H_2O$)**) was localized displaying an energy barrier (ΔG_{gas}) of 25.3 kcal mol^{-1} (or 31.1 kcal mol^{-1} with respect to **L_2-$Int1^T$($2H_2O$)**). Bearing in mind that the initial naked meta-oxo complex **Cat** with one coordinated water molecule (**L_2-$Int1^S$(H_2O)**) presented a more stable singlet ground state over triplet state, and thus there is a strong chance that in the presence of **W_2** molecule the system will go directly to the transition state without being collapsed to triplet complex **L_2-$Int1^S$($2H_2O$)**. In that case it is logical to consider the effective barrier from **L_2-$Int1^S$** to **L_2-TS^S**. From the transition state the system will collapses to peroxo complex **L_2-$Int1^T$($2H_2O$)**, which presented stable singlet ground state and lies 5.0 kcal mol^{-1} above **L_2-$Int1^S$($2H_2O$)** (or 10.8 kcal mol^{-1} above **L_2-$Int1^T$($2H_2O$)**).

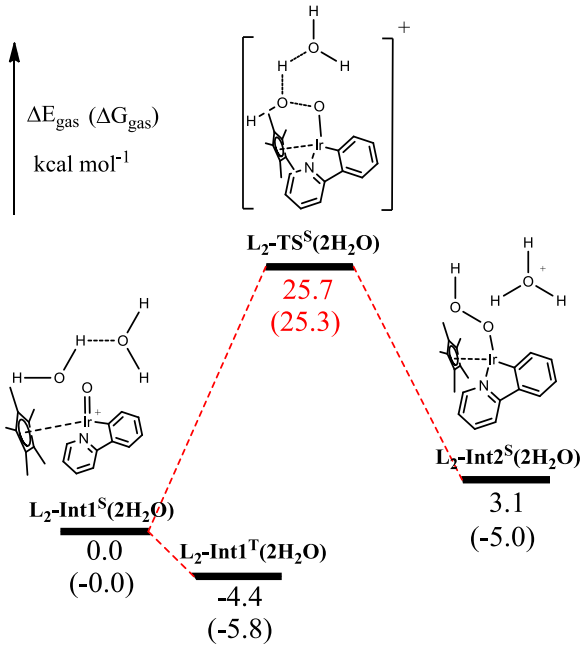

Figure 4. Reaction energy profile for O-O coupling step Cp*Ir-**L_2** catalyst with two water molecules (energies are given in kcal mol^{-1} relative to **L_1-$Int1^S$($2H_2O$)**).

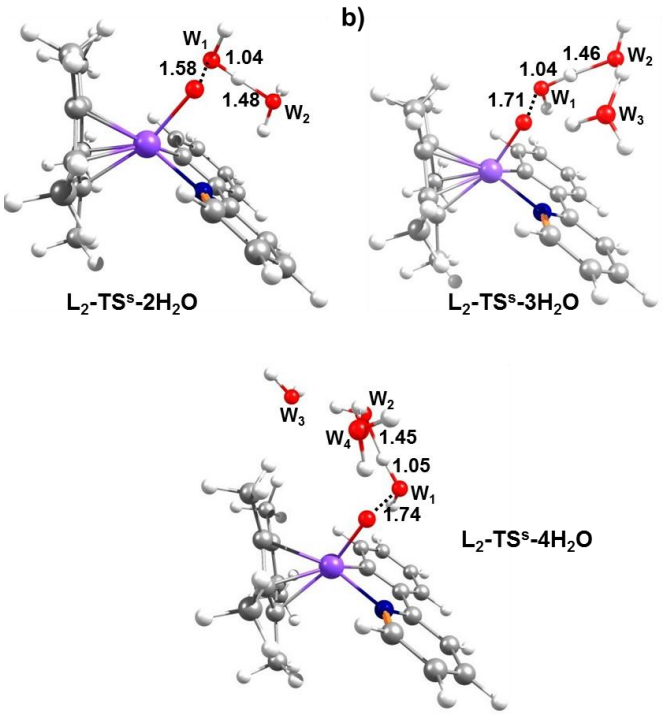

Figure 5. Transition state structures for O-O coupling reaction with 2-4 water molecules for the catalyst Cp*Ir-L_{2-4}. Important bond lengths are given in Å.

Table 3. Relative energies of singlet (S) and triplet (T) ground states of key intermediates of the water oxidation catalytic cycle for the studied iridium catalyst series Cp*Ir-$\mathbf{L}_{x=1-4}$., in the presence of three water molecules (energies are given in kcal mol^{-1}).

	Gas Phase		Solvent-phase	
Species	ΔE_{gas}	ΔG_{gas}	ΔE_{sol}	ΔG_{sol}
L_1-Cat^S	16.7	2.7	10.0	-4.0
L_1-Cat^T	8.8	-6.1	5.3	-9.6
L_1-$Int1^S$	0.0	0.0	0.0	0.0
L_1-$Int1^T$	-2.4	-4.8	-0.6	-3.1
L_1-TS^S	36.3	37.2	40.6	41.5
L_1-$Int2^S$	21.4	23.2	25.8	27.6
L_2-Cat^S	15.1	1.5	8.2	-5.4
L_2-Cat^T	8.2	-7.1	3.1	-12.2
L_2-$Int1^S$	0.0	0.0	0.0	0.0
L_2-$Int1^T$	-2.2	-5.0	-1.3	-4.1
L_2-TS^S	24.4	23.8	27.0	26.4
L_2-$Int2^S$	8.3	8.2	11.6	11.5
L_3-Cat^S	21.1	7.5	6.8	-6.9
L_3-Cat^T	6.6	-7.7	-4.5	-18.7
L_3-$Int1^S$	0.0	0.0	0.0	0.0
L_3-$Int1^T$	-12.9	-19.0	-6.6	-12.7
L_3-TS^S	8.8	8.2	8.7	8.2
L_3-$Int2^S$	-16.5	-17.9	-10.0	-11.4
L_4-Cat^S	15.2	1.7	8.2	-5.2
L_4-Cat^T	7.9	-7.6	2.6	-12.9
L_4-$Int1^S$	0.0	0.0	0.0	0.0
L_4-$Int1^T$	-2.7	-5.4	-1.7	-4.4
L_4-TS^S	23.8	23.5	26.1	25.8
L_4-$Int2^S$	8.8	8.1	11.6	11.0

The catalytic activity of water oxidation catalyst is dependent on the O-O bond formation step, which can bear a different number of associated water molecules in the reactive system. Giving a look at the geometry variations with respect to the number of water molecules, we can distinguish that the corresponding transition state bearing 2 water molecules of the O-O coupling step the O···O distance is 1.58 Å, whereas with 3 water molecules the distance increases to 1.62 Å (see Figure 5). At the same time the distance between the second water molecule to the proton to be abstracted from the first water molecule is also an important factor as it governs the reactivity the hydroxyl moiety of the latter water molecule towards the oxo group.[23] This distance decreases from 1.57, 1.41, to 1.38 Å bearing 2-4 water molecules, respectively, which confirms that the proton abstraction is facilitated with a larger number of water molecules hence the nucleophilic nature of the hydroxyl moiety towards oxo group increases. Actually, the participation of outer-sphere water was first taken into account in water oxidation by Ru polyoxometallates,[24] also bearing proton transfer reactions involving transition metal complexes, which is key here to stabilize the proton released from the water molecule that nucleophilically attacks the oxo species.[25] Even though there is a sharp difference between the second and third water molecules, the fourth water molecule does not significantly affect.

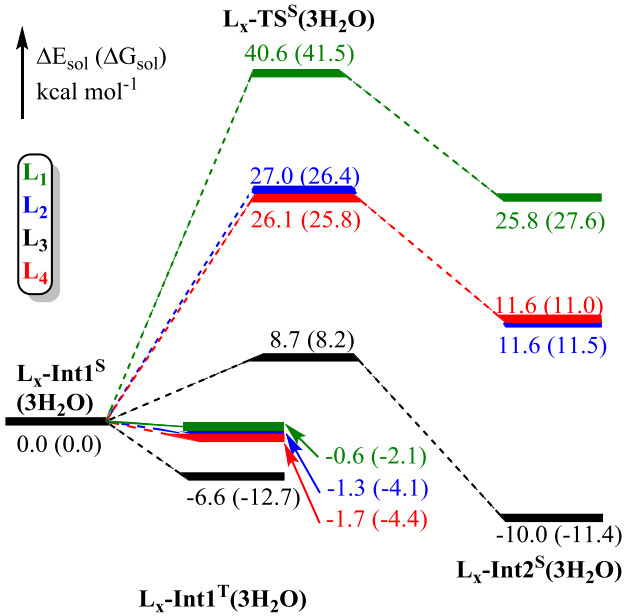

Figure 6. Reaction energy profile for O-O coupling reaction for the studied iridium catalyst series Cp*Ir-$\mathbf{L_{x=1-4}}$ with three water molecules.

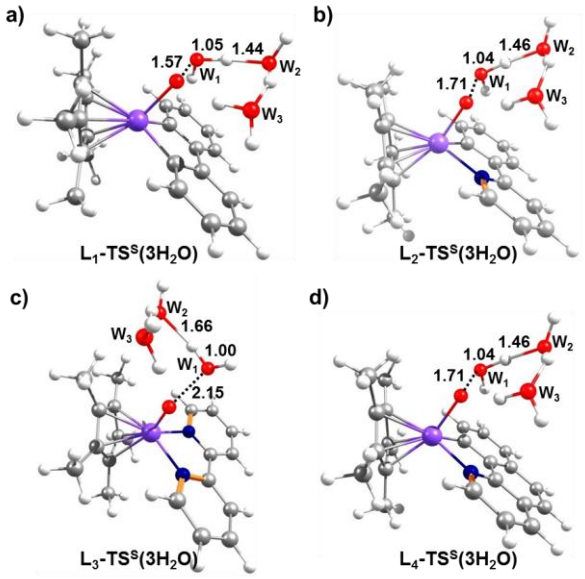

Figure 7. Transition state structures for O-O coupling reaction with three water molecules for the studied Ir catalyst series Cp*Ir-$\mathbf{L_{x=1-4}}$. Main distances are given in Å.

Having described the O-O coupling step is kinetically more favorable with three water molecules, we finally calculated the reaction energy profile for the O-O coupling for the studied catalyst series Cp*Ir-$\mathbf{L_{x=1-4}}$ (Table 3). The selected ligands impose different charges ($\mathbf{L_1}$=0, $\mathbf{L_2}$=+1, $\mathbf{L_3}$=+2 and $\mathbf{L_4}$ =+1) on the metal center of complex $\mathbf{L_x}$-**Cat**, and thus give opportunity to rationalize the catalytic activity as function of charge on the metal center. We considered the energy of the first intermediate in singlet ground state ($\mathbf{L_x}$-**Int1^S(2H$_2$O)**) as the reference.

Among **L1**-**L4** Ir-catalysts, there are substantial differences for the key transition state of the O-O bond formation bearing 3 water molecules (see Figures 6 and 7). Bearing the energy of **INT1^S**, the barrier (ΔG$_{sol}$) decreases from 41.5 kcal mol^{-1} for **L1** to 8.2 kcal mol^{-1} for **L3**, with 26.4 kcal mol^{-1} for **L2** and 25.8 kcal mol^{-1} for **L4** in between. Thus, the higher the electrophilic character on the metal, the lower the barrier is.

Bearing the recent computational studies by Chen, Shaik,[26] Siegbahn and coworkers on a WOC complex,[27] once completed the water nucleophilic attack above, *i.e.* a mononuclear mechanism, we also computed the alternative bimolecular mechanism (see Table 4). The higher the electrophilicity of metal center, the higher the preference for the bimolecular mechanism is. The calculated barrier for system **L3** with triplet ground state is 21.7 kcal mol^{-1} with respect to the triplet ground state of both separated **L3-Cat^T** moieties.

Table 4. Relative energies of singlet (S) and triplet (T) ground states of key intermediates of the O-O bond formation in the bimolecular mechanism for the studied iridium catalyst series Cp*Ir-$\mathbf{L_{x=1-4}}$ in water (energies are given in kcal mol^{-1}).

Species	ΔE$_{sol}$	ΔG$_{sol}$	Species	ΔE$_{sol}$	ΔG$_{sol}$
L$_1$-Cat^S	4.6	5.6	L$_3$-Cat^S	11.3	11.9
L$_1$-Cat^T	0.0	0.0	L$_3$-Cat^T	0.0	0.0
L$_1$-TS^S	17.2	32.6	L$_3$-TS^S	27.7	41.5
L$_1$-TS^T	- [(a)]	- [(a)]	L$_3$-TS^T	11.2	21.7
L$_1$-Int2^S	-5.6	12.9	L$_3$-Int2^S	-18.4	2.2
L$_1$-Int2^T	-5.7	11.4	L$_3$-Int2^T	-15.6	-2.6
L$_2$-Cat^S	5.1	6.8	L$_4$-Cat^S	5.6	7.6
L$_2$-Cat^T	0.0	0.0	L$_4$-Cat^T	0.0	0.0
L$_2$-TS^S	12.8	27.6	L$_4$-TS^S	3.3	19.1
L$_2$-TS^T	- [(a)]	- [(a)]	L$_4$-TS^T	7.8	22.2
L$_2$-Int2^S	-16.5	0.8	L$_4$-Int2^S	-16.5	0.3
L$_2$-Int2^T	-14.7	2.1	L$_4$-Int2^T	-15.6	1.4

(a) Not located

On the other hand, the calculated barrier for the water nucleophilic attack is 32.2 kcal mol^{-1} by taking **L3-Cat^T** as a reference as well. Then the barrier for the biradical singlet for the bimolecular mechanism is 32.6, 27.6 and 19.1 kcal mol^{-1} for systems **L1**, **L2** and **L4**, respectively (see Figure 8). To point out that for **L1** and **L2** the transition state bearing triplet multiplicity was not located, however singlet point energy calculations on the corresponding biradical singlet geometries displayed less stability by at least 7.0 kcal mol^{-1}. Overall, at high concentration of catalyst the bimolecular mechanism becomes favorable or at least highly competitive with

respect to the three-water assisted mononuclear mechanism for **L2** and **L4**.

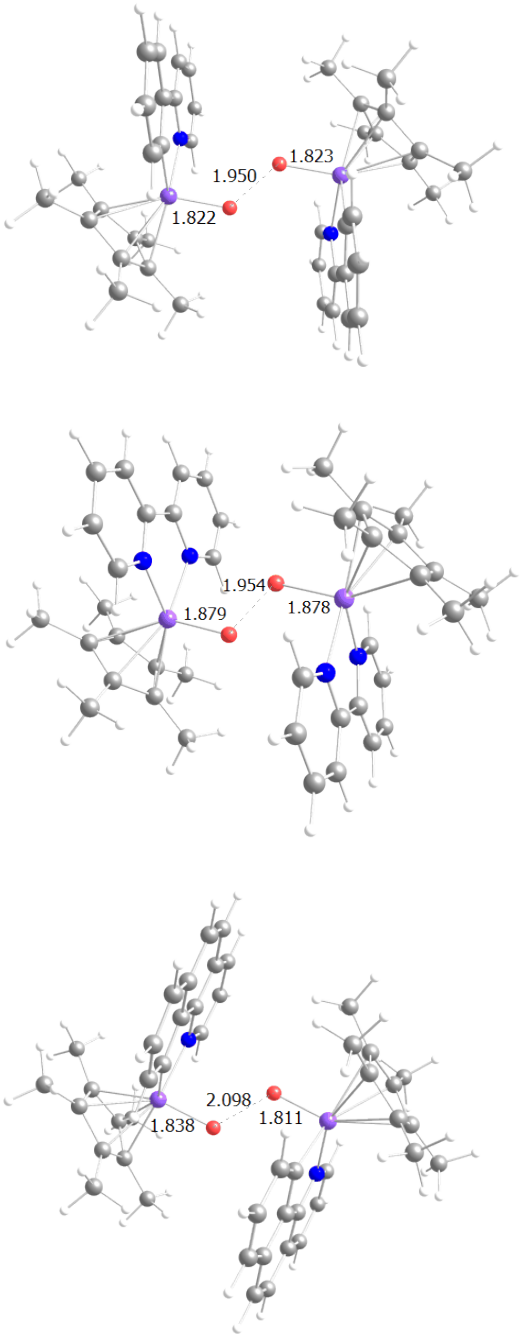

Figure 8. Transition state structures for O-O bond formation for the bimolecular mechanism for the studied catalysts (a) Cp*Ir-$\mathbf{L}_2$, (b) Cp*Ir-$\mathbf{L}_3$, (c) Cp*Ir-$\mathbf{L}_4$. Main distances are given in Å.

Conclusion

The water oxidation catalytic mechanism by Cp*-iridium based complexes has been unraveled by means of DFT calculations. In particular, the current study focuses mainly on the rate determining step that consists of the O-O bond formation. Despite the relative low stability of the studied Cp*-iridium based catalysts,[28] bearing the water nucleophilic attack they give here the basis to explain how the number of water molecules participate actively in the corresponding water assisted transition state. Furthermore the bimolecular mechanism is also studied and put into direct comparison with the unimolecular one. Further, we unravel that the metal environment is more prone to water oxidation catalysis with ligands holding chelation N-N rather than C-C, or C-N. However, the main outcome of this study is that the aqueous carrousel affords the O-O bond through the lowest barrier bearing 3 water molecules, in competition with the bimolecular mechanism at low dilution of catalyst.

Computational Details: The mechanistic aspects of the water oxidation were studied by density functional theory (DFT)[29] using Gaussian 09 package.[30] The PBEh1PBE functional have been used and metals Iridium (Ir), we used the small-core, quasirelativistic Stuttgart/Dresden effective core potential, with the associated valence basis set (SDD).[31] All other atoms (O, C and H) have been represented by triple zeta quality of basis sets TZVP.[32] We have examined the singlet, triplet and quintet spin states for all the species studied. The transition states identification was performed using synchronous transit-guided quasi-Newton (QST3) approach and the extrema have been checked by analytical frequency calculations. In addition, the Intrinsic Reaction Coordinate (IRC) procedure has been used to extrapolate the two minima connected by each transition state. The discussion of the results is based on the total energies which includes electronic energies (E), ZPE corrections and Gibbs free energies (G) at 298.15 K and 1 atm. The G values were computed assuming an ideal gas, unscaled harmonic vibrational frequencies and the rigid rotor approximation. Solvent effects including contributions of non-electrostatic terms have been used based on the polarizable continuum solvation model CPCM.[33,34]

ASSOCIATED CONTENT

Cartesian coordinates for all the compounds. This material is available free of charge via the Internet at http://pubs.acs.org.

AUTHOR INFORMATION

Corresponding Authors
*E-mail: albert.poater@outlook.com, jeanmarie.basset@kaust.edu.sa.
Notes
The authors declare no competing financial interest.

ACKNOWLEDGMENT

The OCRF of King Abdullah University of Science and Technology (KAUST) KSA is acknowledged for the award of CADENCED project under special academic partner IFP-France and KAUST KSA. We thank Prof. Cavallo, Dr. Takanabe, and Dr. Joya for helpful comments. A.P. thanks the Spanish MINECO for a project CTQ2014-59832-JIN.

ABBREVIATIONS

CCR2, CC chemokine receptor 2; CCL2, CC chemokine ligand 2; CCR5, CC chemokine receptor 5; TLC, thin layer chromatography.

REFERENCES

[1] (a) Blakemore, J. D.; Crabtree, R. H.; Brudvig, G. W. Chem. Rev. 2015, 115, 12974–13005. (b) Molecular Water Oxidation Catalysis: A Key Topic for New Sustainable Energy Conversion Schemes (Ed.: A. Llobet), Wiley, Hoboken, 2014, ISBN:9781118413371. (c) McEvoy, J. P.; Brudvig, G. W. *Chem. Rev.* **2006**, *106*, 4455-4483. (d) Dau, H.; Limberg, C.; Reier, T.; Risch, M.; Roggan, S.; Strasser, P. *ChemCatChem* **2010**, *2*, 724-761. (e) Ferreira, K. N.; Iverson, T. M.; Maghloaoui, K.; Barber, J.; Iwata, S. *Science* **2001**, *303*, 1831-1838. (f) Karkas, M. D.; Verho, O.; Johnston, E. V.; Akermark, B. *Chem. Rev.* **2015**, *114*, 11863-12001.

[2] (a) Youngblood, W. J.; Lee, S. H. A.; Kobayashi, Y.; Hernandez-Pagan, E. A.; Hoertz, P. G.; Moore, T. A.; Moore, A. L.; Gust, D.; Mallouk, T. E. *J. Am. Chem. Soc.* **2009**, *131*, 926-927. (b) Gust, D.; Moore, T. A.; Moore, A. L. *Acc. Chem. Res.* **2009**, *42*, 1890-1898. (c) Hurst, J. K. *Science* **2010**, *328*, 315-316. (d) Lloret-Fillol, J.; Codolà, Z.; Garcia-Bosch, I.; Gómez, L.; Pla, J. J.; Costas, M. *Nat. Chem.* **2011**, *3*, 807-813.

[3] Rüttinger, W.; Dismukes, G. C. *Chem. Rev.* **1997**, *97*, 1-24.

[4] (a) Grätzel, M. *Nature* **2001**, *414*, 338-344. (b) Ueda, K.; Minegishi, T.; Clune, J.; Nakabayashi, M.; Hisatomi, T.; Nishiyama, H.; Katayama, M.; Shibata, N.; Kubota, J.; Yamada, T.; Domen, K. *J. Am. Chem. Soc*. **2015**, *137*, 2227-2230.

[5] (a) Kanady, J. S.; Tsui, E. Y.; Day, M. W.; Agapie, T. *Science* **2011**, *333*, 733-736. (b) Sartorel, A.; Carraro, M.; Scorrano, G.; De Zorzi, R.; Geremia, S.; McDaniel, N. D.; Bernhard, S.; Bonchio, M. *J. Am. Chem. Soc.* **2008**, *130*, 5006-5007. (c) Geletii, Y. V.; Botar, B.; Koegerler, P.; Hillesheim, D. A.; Musaev, D. G.; Hill, C. L. *Angew. Chem. Int. Ed.* **2008**, *47*, 3896-3899. (d) Kanan, M. W.; Nocera, D. G. *Science* **2008**, *321*, 1072-1075. (e) Yin, Q. S.; Tan, J. M.; Besson, C.; Geletii, Y. V.; Musaev, D. G.; Kuznetsov, A. E.; Luo, Z.; Hardcastle, K. I.; Hill, C. L. *Science* **2010**, *328*, 342-345. (f) Reece, S. Y.; Hamel, J. A.; Sung, K.; Jarvi, T. D.; Esswein, A. J.; Pijpers, J. J. H.; Nocera, D. G. *Science* **2011**, *334*, 645-648.

[6] (a) Limburg, B.; Bouwman, E.; Bonnet, S. *Coord, Chem. Rev.* **2012**, *256*, 1451-1467. (b) Cao, R.; Lai, W. Z.; Du, P. W. *Energy Environ. Sci.* **2012**, *5*, 8134-8157.

[7] (a) Romain, S.; Vigara, L.; Llobet, A. *Acc. Chem. Rev.* **2009**, *42*, 1944-1953. (b) Concepcion, J. J.; Jurss, J. W.; Brennaman, M. K.; Hoertz, P. G.; Patrocinio, A. O. T.; Iha, N. Y. M.; Templeton, J. L.; Meyer, T. J. *Acc. Chem. Rev.* **2009**, *42*, 1954-1965. (c) Sens, C.; Romero, I.; Rodriguez, M.; Llobet, A.; Parella, P.; Benet-Buchholz, J. *J. Am. Chem. Soc.* **2004**, *126*, 7798-7799. (d) Gilbert, J. A.; Eggleston, D. S.; Murphy, W. R.; Geselowitz, D. A.; Gersten, S. W.; Hodgson, D. J.; Meyer, T. J. *J. Am. Chem. Soc.* **1985**, *107*, 3855-3864. (e) Concepcion, J. J.; Jurss, J. W.; Templeton, J. L.; Meyer, T. J. *J. Am. Chem. Soc.* **2008**, *130*, 16462-16463.

[8] (a) Sala, X.; Romero, I.; Rodriguez, M.; Escriche, L.; Llobet, A. *Angew. Chem., Int. Ed.* **2009**, *48*, 2842-2852. (b) Duan, L. L.; Fischer, A.; Xu, Y. H.; Sun, L. C. *J. Am. Chem. Soc.* **2009**, *131*, 10397-10398. (c) Hurst, J. K.; Cape, J. L.; Clark, A. E.; Das, S.; Qin, C. Y. *Inorg. Chem.* **2008**, *47*, 1753-1764. (d) Concepcion, J. C.; Jurss, J. W.; Norris, M. R.; Chen, Z.; Templeton, J. L.; Meyer, T. J. *Inorg. Chem.* **2010**, *49*, 1277-1279. (e) Richmond, C. J.; Matheu, R.: Poater, A.; Falivene, L.; Benet-Buchholz, J.; Sala, X.; Cavallo, L.; Llobet, A. *Chem. Eur. J.* **2014**, 20, 17282-17286. (f) Duan, L.; Wang, L.; Inge, A. K.; Fischer, A.; Zou, X.; Sun, L. *Inorg. Chem.* **2013**, *52*, 7844-7852. (g) Duan, L.; Bozoglian, F.; Mandal, S.; Stewart, B.; Privalov, T.; Llobet, A.; Sun, L. *Nat. Chem.* **2012**, *4*, 418-423. (h) Poater, A. *Catal. Commun.* **2014**, *44*, 2-5. (i) Matheu, R.; Ertem, M. Z.; Benet-Buchholz, J.; Coronado, E.; Batista, V. S.; Sala, X.; Llobet, A. *J. Am. Chem. Soc.* **2015**, *137*, 10786-10795.

[9] McDaniel, N. D.; Coughlin, F. J.; Tinker, L. L.; Bernhard, S. *J. Am. Chem. Soc.* **2008**, *130*, 210-217.

[10] Hull, J. F.; Balcells, D.; Blakemore, J. D.; Incarvito, C. D.; Eisenstein, O.; Brudvig, G. W.; Crabtree, R. H. *J. Am. Chem. Soc.* **2009**, *131*, 8730-8731.

[11] Grotjahn, D. B.; Brown, D. B.; Martin, J. K.; Marelius, D. C.; Abadjian, M. C.; Tran, H. N.; Kalyuzhny, G.; Vecchio, K. S.; Specht, Z. G.; Cortes-Llamas, S. A.; Miranda-Soto, V.; van Niekerk, C.; Moore, C. E.; Rheingold, A. L. *J. Am. Chem. Soc.* **2011**, *133*, 19024-19027.

[12] Joya, K. S.; Subbaiyan, N. K.; D'Souza, F.; de Groot, H. J. M. *Angew. Chem. Int. Ed.* **2012**, *51*, 9601-9605.

[13] Pastori, G.; Wahab, K.; Bucci, A.; Bellachioma, G.; Zuccaccia, C.; Llorca, J.; Idriss, H.; Macchioni, A. *Chem. Eur. J.* **2016**, *22*, 13459-13463.

[14] (a) Savini, A.; Bellachioma, G.; Ciancaleoni, G.; Zuccaccia, C.; Zuccaccia, D.; Macchioni, A. *Chem. Commun.* **2015**, *46*, 9218-9219. (b) Savini, A.; Belanzoni, P.; Bellachioma, G.; Ciancaleoni, G.; Zuccaccia, C.; Zuccaccia, D.; Macchioni, A. *Green Chem.* **2011**, *13*, 3360-3374. (c) Savini, A.; Bucci, A., Bellachioma, G.; Rocchigiani, L.; Zuccaccia, C.; Llobet, A.; Macchioni, A. *Eur. J. Inorg. Chem.* **2014**, 690-697. (d) Savini, A.; Bucci, A.; Bellachioma, G.; Giancola, S.; Palomba, F.; Rocchigiani, L.; Rossi, A.; Suriani, M.; Zuccaccia, C.; Macchioni, A. *J. Organomet. Chem.* **2014**, *771*, 24-32. (e) Corbucci, I.; Petronilho, A.; Muller-Bunz, H.; Rocchigiani, L.; Abrecht, M.; Macchioni, A. *ACS Catal.* **2015**, 5, 2714-2718. (f) Broeckx, L. E. E.; Bucci, A.; Zuccaccia, C.; Lutz, M.; Macchioni, A.; Muller, C. *Organometallics* **2015**, *34*, 2943-2952.

[15] (a) Joya, K. S.; Joya, Y. F.; Ocakoglu, K.; van de Krol, R. *Angew. Chem. Int. Ed*. **2013**, 52, 10426-10437. (b) Joya, K. S.; de Groot, H. J. M. *Int. J. Hydrogen Energy* **2012**, *37*, 8787-8799. (c) Vallés-Pardo, J. L.; Guijt, M. C.; Iannuzzi, M.; Joya, K. S.; de Groot, H. J. M.; Buda, F. *ChemPhysChem* **2012**, *13*, 140-146. (d) Joya, K. S.; Vallés-Pardo, J. L.; Joya, Y. F.; Eisenmayer, T.; Thomas, B.; Buda, F.; de Groot, H. J. M. *ChemPlusChem* **2013**, *78*, 35-47.

[16] (a) Brudvig, G. W.; Crabtree, R. H. *Proc. Natl. Acad. Sci. U.S.A.* **1986**, *83*, 4586-4588. (b) Brudvig, G. W. *Phil. Trans. R. Soc. B* **2008**, *363*, 1211-1219. (c) Brudvig, G. W.; Thorp, H. H.; Crabtree, R. H. *Acc. Chem. Res.* **1991**, *24*, 311-316. (d) Neudeck, S.; Maji, S.; López, I.; Meyer, S.; Meyer, F.; Llobet, A. *J. Am. Chem. Soc.* **2014**, *136*, 24-27. (e) López, I.; Ertem, M. Z.; Maji, S.; Benet-Buchholz, J.; Keidel, A.; Kuhlmann, U.; Hildebrandt, P.; Cramer, C. J.; Batista, V. S.; Llobet, A. *Angew. Chem. Int. Ed.* **2014**, *53*, 205-210. (f) Acuña-Parés, F.; Codolà, Z.; Costas, M.; Luis, J. M.; Lloret-Fillol, J. *Chem. Eur. J.* **2014**, *20*, 5696-5707. (g) Acuña-Parés, F.; Costas, M.; Luis, J. M.; Lloret-Fillol, J. *Inorg. Chem.* **2014**, 53, 5474-5485. (h) To, W. P.; Chow, T. W. S.; Tse, C. W.; Guan, X. G.; Huang, J. S.; Che, C. M. *Chem. Sci.* **2015**, *6*, 5891-5903.

[17] (a) Petronilho, A.; Rahman, M.; Woods, J. A.; Al-Sayyed, H.; Müller-Bunz, H.; Don MacElroy, J. M.; Bernhard, S.; Albrecht, M. *Dalton Trans.* **2012**, *41*, 13074-13080. (b) Petronilho, A.; Llobet, A.; Albrecht, M. *Inorg. Chem.* **2014**, *53*, 12896-12901. (c) Corbucci, I.; Petronilho, A.; Müller-Bunz, H.; Rocchigiani, L.; Albrecht, M.; Macchioni, A. *ACS Catal.* **2015**, *5*, 2714-2718.

[18] (a) Graeupner, J.; Hintermair, U.; Huang, D. L.; Thomsen, J. M.; Takase, M.; Campos, J.; Hashmi, S. M.; Elimelech, M.; Brudvig, G. W.; Crabtree, R. H. *Organometallics* **2013**, *32*, 5384-5390. (b) Ingram, A. J.; Wolk, A. B.; Flender, C.; Zhang, J. L.; Johnson, C. J.; Hintermair, U.; Crabtree, R. H.; Johnson, M. A.; Zare, R. N. *Inorg. Chem.* **2014**, *53*, 423-433. (c) Thomsen, J. M.; Sheehan, S. W.; Hashmi, S. M.; Campos, J.; Hintermair, U.; Crabtree, R. H.; Brudvig, G. W. *J. Am. Chem. Soc.* **2014**, *136*, 13826-13834. (d) Thomsen, J. M.; Huang, D. L.; Crabtree, R. H.; Brudvig, G. W. *Dalton Trans.* **2015**, *44*, 12452-12472.

[19] Bucci, A.; Menendez Rodriguez, G.; Bellachioma, G.; Zuccaccia, C.; Poater, A.; Cavallo, L.; Macchioni, A. *ACS Catal.* **2016**, *6*, 4559-4563.

[20] (a) Sartorel, A.; Miro, P.; Salvadori, E.; Romain, S.; Carraro, M.; Scorrano, G.; Di Valentin, M.; Llobet, A.; Bo, C.; Bonchio, M. *J. Am. Chem. Soc.* **2009**, *131*, 16051-16053. (b) Kohl, S. W.; Weiner, L.; Schwartsburd, L.; Konstantinovski, L.; Shimon, L. J. W.; Ben-David, Y.; Iron, M. A.; Milstein, D. *Science* **2009**, *324*, 74-77. (c) Geletii, Y. V.; Besson, C.; Hou, Y.; Yin, Q.; Musaev, D. G.; Quiñonero, D.; Cao, R.; Hardcastle, K. I.; Proust, A.; Kögerler, P.; Hill, C. L. *J. Am. Chem. Soc.* **2009**, *131*, 17360-17370. (d) Chen, Z. F.; Concepcion, J. J.; Hu, X. Q.; Yang, W. T.; Hoertz, P. G.; Meyer, T. J. *Proc. Natl. Acad. Sci. U.S.A.* **2010**, *107*, 7225-7229. (e) Wang, L.-P.; Wu, Q.; Voorhis, T. V. *Inorg. Chem.* **2010**, *49*, 4543-4553. (f) Geletii, Y. V.; Huang, Z.; Hou, Y.; Musaev, D. G.; Lian, T.; Hill, C. L. *J. Am. Chem. Soc.* **2009**, *131*, 7522-7523.

[21] Kazaryan, A.; van Santen, R.; Baerends, E. J. *Phys. Chem. Chem. Phys.* **2015**, *17*, 20308-20321.

[22] Blakemore, J. D.; Schley, N. D.; Balcells, D.; Hull, J. F.; Olack, G. W.; Incarvito, C. D.; Eisenstein, O.; Brudvig, G. W.; Crabtree, R. H. *J. Am. Chem. Soc.* **2010**, *132*, 16017-16029.

[23] (a) Li, J.; Shiota, Y.; Yoshizawa, K. *J. Am. Chem. Soc.* **2009**, *131*, 13584-13585. (b) Yang, X.; Hall, M. B. *J. Am. Chem. Soc.* **2010**, *132*, 120-130.

[24] Kuznetsov, A. E.; Geletii, Y. V.; Hill, C. L.; Morokuma, K.; Musaev, D. G. *J. Am. Chem. Soc.* **2009**, *131*, 6844-6854.

[25] (a) Filippov, O. A.; Filin, A. M.; Tsupreva, V. N.; Belkova, N. V.; Lledós, A.; Ujaque, G.; Epstein, L. M.; Shubina, E. S. *Inorg. Chem.* **2006**, *45*, 3086-3096. (b) Filippov, O. A.; Tsupreva, V. N.; Golubinskaya, L. M.; Krylova, A. I.; Bregadze, V. I.; Lledós, A.; Epstein, L. M.; Shubina, E. S. *Inorg. Chem.* **2009**, *48*, 3667-3678.

[26] Kang, R. H.; Chen, K. J.; Yao, J. N. A.; Shaik, S.; Chen, H. Inorg. Chem. **2014**, *53*, 7130-713.

[27] Liao, R.-Z.; Siegbahn, P. E. M. *ACS Catal.* **2014**, *4*, 3937-3949.

[28] (a) Crabtree, R. H. *J. Organomet. Chem.* **2014**, *751*, 174-180. (b) Campos, J.; Hintermair, U.; Brewster, T. P.; Takase, M. K.; Crabtree, R. H. *ACS Catal.* **2014**, *4*, 973-985.

[29] Parr, R. G.; Weitao, Y. *Density-functional theory of atoms and molecules*; Oxford University Press, 1994.

[30] Gaussian 09, Revision D.01, Frisch, M. J.; Trucks, G. W.; Schlegel, H. B.; Scuseria, G. E.; Robb, M. A.; Cheeseman, J. R.; Scalmani, G.; Barone, V.; Mennucci, B.; Petersson, G. A.; Nakatsuji, H.; Caricato, M.; Li, X.; Hratchian, H. P.; Izmaylov, A. F.; Bloino, J.; Zheng, G.; Sonnenberg, J. L.; Hada, M.; Ehara, M.; Toyota, K.; Fukuda, R.; Hasegawa, J.; Ishida, M.; Nakajima, T.; Honda, Y.; Kitao, O.; Nakai, H.; Vreven, T.; Montgomery, J. A., Jr.; Peralta, J. E.; Ogliaro, F.; Bearpark, M.; Heyd, J. J.; Brothers, E.; Kudin, K. N.; Staroverov, V. N.; Kobayashi, R.; Normand, J.; Raghavachari, K.; Rendell, A.; Burant, J. C.; Iyengar, S. S.; Tomasi, J.; Cossi, M.; Rega, N.; Millam, J. M.; Klene, M.; Knox, J. E.; Cross, J. B.; Bakken, V.; Adamo, C.; Jaramillo, J.; Gomperts, R.; Stratmann, R. E.; Yazyev, O.; Austin, A. J.; Cammi, R.; Pomelli, C.; Ochterski, J. W.; Martin, R. L.; Morokuma, K.; Zakrzewski, V. G.; Voth, G. A.; Salvador, P.; Dannenberg, J. J.; Dapprich, S.; Daniels, A. D.; Farkas, Ö.; Foresman, J. B.; Ortiz, J. V.; Cioslowski, J.; Fox, D. J. Gaussian, Inc., Wallingford CT, 2009.

[31] (a) Leininger, T.; Nicklass, A.; Stoll, H.; Dolg, M.; Schwerdtfeger, P. *J. Chem. Phys.* **1996**, *105*, 1052-1059. (b) Kuchle, W.; Dolg, M.; Stoll, H.; Preuss, H. *J. Chem. Phys.* **1994**, *100*, 7535-7542. (c) Haussermann, U.; Dolg, M.; Stoll, H.; Preuss, H.; Schwerdtfeger, P.; Pitzer, R. M. *Mol. Phys.* **1993**, *78*, 1211-1224.

[32] (a) Schafer, A.; Horn, H.; Ahlrichs, R. *J. Chem. Phys.* **1992**, *97*, 2571-2577. (b) Schafer, A.; Huber, C.; Ahlrichs, R. *J. Chem. Phys.* **1994**, *100*, 5829-5835.

[33] (a) Barone, V.; Cossi, M. *J. Phys. Chem. A* **1998**, *102*, 1995-2001. (b) Cossi, M.; Rega, N.; Scalmani, G.; Barone, V. *J. Comput. Chem.* **2003**, *24*, 669-681.

[34] Tomasi, J.; Persico, M. *Chem. Rev.* **1994**, *94*, 2027-2094.

TOC

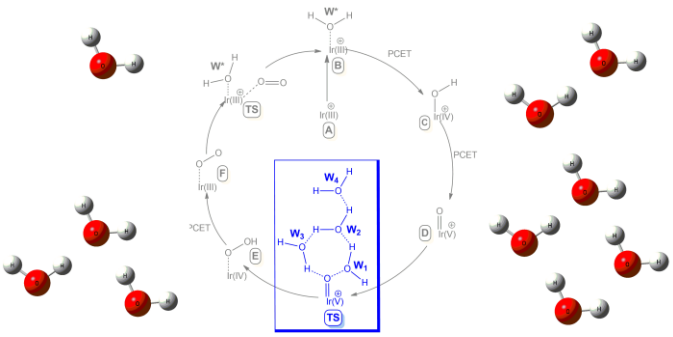

Bimolecular system vs water molecules assisting the O-O bond formation in water oxidation catalysis by a Cp*-Ir based family of complexes